Letter

Random matrix theory for quantum and classical metastability in local Liouvillians

Jimin L. Li,[1] Dominic C. Rose,[2,3,4] Juan P. Garrahan,[2,3] and David J. Luitz[5]

[1]*Department of Chemistry, University of Cambridge, Lensfield Road, Cambridge CB2 1EW, United Kingdom*
[2]*School of Physics and Astronomy, University of Nottingham, Nottingham NG7 2RD, United Kingdom*
[3]*Centre for the Mathematics and Theoretical Physics of Quantum Non-Equilibrium Systems, University of Nottingham, Nottingham NG7 2RD, United Kingdom*
[4]*Department of Physics and Astronomy, University College London, Gower Street, London WC1E 6BT, United Kingdom*
[5]*Max Planck Institute for the Physics of Complex Systems, Noethnitzer Straße 38, 01187 Dresden, Germany*

(Received 9 November 2021; revised 13 April 2022; accepted 18 April 2022; published 6 May 2022)

We consider the effects of strong dissipation in quantum systems with a notion of locality, which induces a hierarchy of many-body relaxation timescales as shown by K. Wang, F. Piazza, and D. J. Luitz [Phys. Rev. Lett. **124**, 100604 (2020)]. If the strength of the dissipation varies strongly in the system, additional separations of timescales can emerge, inducing a manifold of metastable states, to which observables relax first, before relaxing to the steady state. Our simple model, involving one or two "good" qubits with dissipation reduced by a factor $\alpha < 1$ compared to the other "bad" qubits, confirms this picture and admits a perturbative treatment.

DOI: 10.1103/PhysRevB.105.L180201

Introduction. Quantum many-body systems are generically complex, and obtaining an analytic understanding of the position of all spectral resonances is often hopeless. It was realized early on [1–6] that this complexity is in fact so great that many statistical properties of the spectrum are identical with those of random matrices sampled from an ensemble determined by the symmetry of the system. These pioneering observations have been subsequently refined, resulting in cornerstones of our understanding of thermalization in unitary quantum many-body systems by virtue of the eigenstate thermalization hypothesis [7–14], only with exceptions in integrable [15–18], many-body localized [19–29], time-crystalline [30–32], or scarred and constrained systems [33–35].

This thinking was recently pushed to the realm of open quantum systems, with random matrix models of Markovian dissipation defined via random Liouvillians [36–40], revealing fascinating spectral features of generic purely dissipative systems, in particular a spectral support which has the shape of a "lemon" [36,37], very different from the circular spectrum of non-Hermitian Ginibre random matrices [41]. This feature is also present in classical master equations, where typical transition rate matrices have a similar spectral support [42,43].

Such random matrix models of open quantum many-body systems represent the behavior of typical systems, rather than of a specific model. While they reproduce global properties of more realistic, microscopic models, they miss a crucial ingredient: the locality of (dissipative) interactions. It was recently shown that random matrix models for local Liouvillians can be devised exhibiting a hierarchy of relaxation timescales [44]. These models limit the jump operators in the Lindblad equation to low-complexity Pauli strings, thus encoding few-body interactions. In the absence of detailed microscopic knowledge, this accurately models dissipation in current quantum computer prototypes, and the predicted timescales were in fact observed experimentally on the IBM platform [45].

Here we apply such a local random matrix model approach to systems with strongly varying dissipation. We are specifically interested in the appearance of metastable states due to a separation of timescales caused by fast and slow dissipation modes in the system, which we model by the existence of good qubits with low dissipation rates in a system of otherwise bad qubits where dissipation is fast. In this setup a *metastable manifold* (MM) emerges [46], to which the dynamics starting from an arbitrary initial state relaxes quickly. At intermediate times, the dynamics is effectively restricted to the MM, before eventual relaxation to the global steady state at long times. We argue that this model contains the essence of the physics to be expected in a quantum computer with good and bad qubits and is furthermore the simplest generic model to study metastability. Our model generalizes findings of MMs in the presence of local loss terms [47,48].

Model. We construct a simple model for a purely dissipative, Markovian quantum many-body system consisting of ℓ qubits. The Hilbert space dimension is $N = 2^\ell$, and the operator space is spanned by all $N^2 = 4^\ell$ normalized Pauli strings,

$$S_\mu = N^{-1/2}\sigma_{\mu_1} \otimes \sigma_{\mu_2} \otimes \cdots \otimes \sigma_{\mu_\ell}, \quad \mu_i \in \{0, x, y, z\}, \quad (1)$$

where $\sigma_0 = \mathbb{1}$, and $\sigma_{x,y,z}$ are the Pauli matrices. Dissipation is generated by a set of k-local jump operators given by k-local Pauli strings such that the number of nonidentity Pauli matrices in the string is at most k. That is, for k-local S_μ we have $\sum_{i=1}^{l}(1 - \delta_{\mu_i,0}) \leqslant k$. We will focus on the physically relevant case of two-body dissipative interactions, including

one-qubit and two-qubit ($k = 2$) dissipation channels, yielding $N_L = 3\ell + 9\binom{\ell}{2}$ jump operators.

The dynamics of the density matrix ρ is governed by the purely dissipative Liouvillian [49] defined in terms of a Kossakowski matrix $K_{\mu\nu}$ which encodes the nontrivial couplings between the dissipation channels and is randomly sampled from the ensemble of *positive-semidefinite* matrices. The sums μ, ν run over the N_L jump operators $L_\mu = S_\mu$, given by k-local Pauli strings in Eq. (1),

$$\mathcal{L}[\rho] = \sum_{\mu,\nu=1}^{N_L} K_{\mu\nu}\left[L_\mu \rho L_\nu^\dagger - \frac{1}{2}\{L_\nu^\dagger L_\mu, \rho\}\right]. \tag{2}$$

Using the same procedure as in Refs. [36,44,45], we generate the i.i.d. non-negative eigenvalues of K from a uniform distribution, and normalize them such that $\mathrm{Tr}K = N$. Then, we rotate the basis by a Haar random unitary $U \in \mathrm{CUE}(N_L)$ to yield $K = U^\dagger D U$, where D is the diagonal eigenvalue matrix of K.

In contrast to Ref. [44], we are interested in understanding the effect of a strongly varying dissipation strength across the system. The simplest way to consider this is by splitting the set of jump operators $\{L_\mu\}$ into *strongly* dissipative ones, $\{L_\mu^{\mathrm{s}}\}$, and *weakly* dissipative ones, $\{L_\mu^{\mathrm{w}}\}$. This is achieved by defining a set of "good" qubits in a system of otherwise "bad" qubits: weak jump operators are those that contain a nonidentity Pauli matrix on a good qubit, so that dissipation happens at a rate scaled by $\sqrt{\alpha} < 1$, $L_\mu^{\mathrm{w}} = \sqrt{\alpha} S_\mu$, while strong jump operators are still of the form $L_\mu^{\mathrm{s}} = S_\mu$ [50].

Spectrum of the Liouvillian. In Fig. 1, we show the complex eigenvalues λ_i of a realization of the Liouvillian for $\ell = 6$, for one (left) and two (right) good qubits, with two-qubit interactions and one-qubit dissipation ($k = 2$-local in our definition). The Liouvillian (2) is bistochastic (as all L_μ are Hermitian); thus it generically has a single eigenvalue zero with the identity as the unique stationary state, and all other eigenvalues with negative real parts.

Due to the locality of our model, the spectrum separates into multiple eigenvalue clusters, organized by the locality of their eigenmodes. If good and bad qubits have the same rate of dissipation ($\alpha = 1$), we recover the spectrum of Ref. [44]. As we make good qubits better ($\alpha < 1$), additional eigenvalue clusters appear. These clusters have a real part proportional to α, and are indicated by the blue bars in Fig. 1. For decreasing α, these clusters move progressively closer to zero. For small α they combine to form the MM (see below) of long-lived states with the slowest relaxation. The other clusters also move slightly with α, but reach a limiting position well separated from the MM.

Note that in the case of one good qubit, there is a single cluster of three eigenvalues close to zero, while for two good qubits there are two such clusters, one with six and the other with nine eigenvalues. To elucidate these spectral properties further, we study these clusters using perturbation theory.

Perturbation theory. Due to the physical requirement that the Liouvillian is trace preserving and completely positive, the random K matrix is diagonally dominant [44]. It hence has the following properties: the mean of the matrix elements $K_{\mu\nu}$ is $\delta_{\mu,\nu} N/N_L$ and the standard deviation is $N/(\sqrt{6} N_L^{3/2})$, which can be shown by the central limit theorem and using random

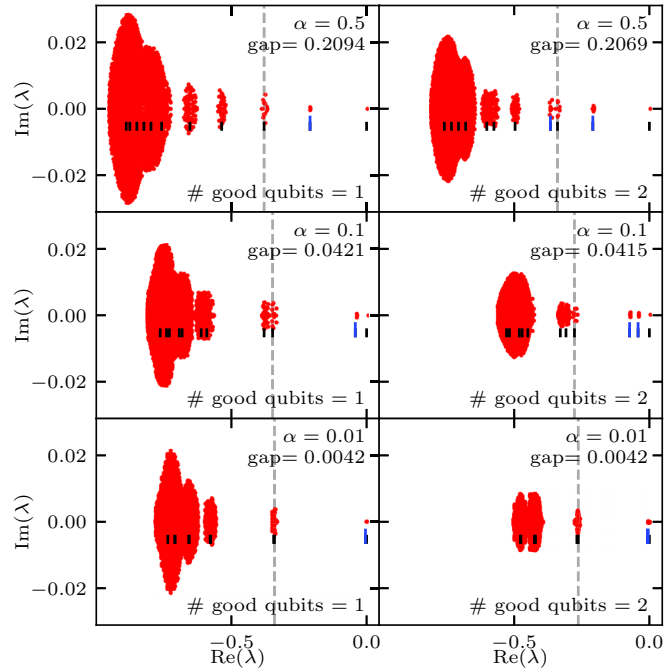

FIG. 1. Spectra λ_i of random local Liouvillians for $\ell = 6$ with one (left column) or two (right column) good qubits as a function of the weak dissipation rate α. The spectral gap, given by the magnitude of the real part of the first excited eigenvalue, decreases proportionally with α. Bars indicate the eigenvalues of the unperturbed Liouvillian $\mathcal{L}^0$, the starting point of our perturbation theory. Blue bars indicate the position of eigenvalues giving rise to the MM at small α. For small α there is a separation between metastable eigenmodes and the rest of the spectrum, since all other eigenvalues have real parts smaller than $\lambda(n_{\mathrm{s}} = 1, n_{\mathrm{w}} = 0)$ given in Eq. (4), and indicated by the vertical dashed line in each panel.

matrix theory for U. Hence, we can devise a perturbative treatment by splitting the K matrix as $K = K_0 + K_1$, where $K_0 = (N/N_L)\mathbb{1}$ is the unperturbed matrix, and K_1 a small perturbation which we neglect for now.

We can express the Liouvillian L (or it adjoint) as a matrix in the Pauli string basis [51] with matrix elements $\mathsf{L}^0_{\mu\nu} = \mathrm{Tr}(S_\mu \mathcal{L}[S_\nu])$. To leading order off-diagonal matrix elements vanish, and by separating the expressions for weak and strong channels we get for the diagonal elements, and thus eigenvalues to leading order,

$$\mathsf{L}^0_{\mu\mu} = -\frac{2}{N_L}\left(\alpha N_\mu^{\mathrm{w}} + N_\mu^{\mathrm{s}}\right), \tag{3}$$

where N_μ^{w} and N_μ^{s} are the numbers of weak and strong jump operators, respectively, that anticommute with S_μ. The numbers n_{w} and n_{s} of nonidentity Pauli matrices on good and bad qubits determine the above. For the 2-local case with ℓ_{w} good qubits, we obtain from Eq. (3)

$$\lambda(n_s, n_w) = -\frac{2}{N_L}\big[6 n_{\mathrm{s}}\ell + 6 n_{\mathrm{s}}\ell_{\mathrm{w}}(\alpha - 1) - 4n_{\mathrm{s}}^2 + \alpha\big(6 n_{\mathrm{w}}\ell - 8 n_{\mathrm{w}} n_{\mathrm{s}} - 4 n_{\mathrm{w}}^2\big)\big]. \tag{4}$$

Since there are many Pauli strings with the same numbers of n_{w} and n_{s}, each eigenvalue is highly degenerate. There

is a unique steady state, $n_w = n_s = 0$, corresponding to the identity.

Including the small perturbation K_1 lifts the degeneracy of the eigenvalues, and gives them small imaginary parts. To see this, we diagonalize the Liouvillian with $K = K_1$ inside each degenerate subspace. Lowly degenerate eigenvalues, which are well separated from the rest of the spectrum, develop into the clusters observed in Fig. 1, while for eigenvalues close to others and with high degeneracy the separation does not survive, and the perturbation theory breaks down in these cases (see [52] for a detailed discussion of this for large systems). For small α, the perturbation theory is excellent and yields well-separated eigenvalue clusters close to the steady state, as can be seen in Fig. 1. Each eigenvalue cluster in this case is centered around the unperturbed eigenvalue $\lambda(n_s, n_w)$, indicated by black ($n_s > 0$) and blue ($n_s = 0$) bars, as predicted from our perturbation theory.

Further inspection of Eq. (4) reveals that eigenvalues corresponding to observables with only identities on bad qubits (i.e., $n_s = 0$) are proportional to $-\alpha$, while any observable with a nonidentity on a bad qubit picks up a constant offset and thus generically has a much faster decay rate. This is what makes up the MM: eigenvalues with real parts proportional to $-\alpha$ are close to zero for small α, and well separated from the rest of the spectrum. They are centered around $\lambda(n_s = 0, n_w) = -\frac{4\alpha}{N_L}(3n_w\ell - 2n_w^2)$, which means that for one good qubit we get one eigenvalue cluster (since n_w can only be either zero or 1), and for ℓ_w good qubits, we get ℓ_w separate eigenvalue clusters with eigenvalues proportional to $-\alpha$. The remaining eigenvalues are always smaller than $\lambda(n_s = 1, n_w = 0) = -\frac{4}{N_L}(3(\ell - \ell_w) - 2 + 3\ell_w\alpha)$, indicated by the vertical dashed line in Fig. 1. This sets the separation between the MM and the rest of the spectrum, and thus the relaxation timescale of an arbitrary initial state toward the MM before relaxation to the steady state happens on a timescale $\propto 1/\alpha$.

Metastable manifold. The existence of eigenvalues with small real parts, which are well separated from the rest of the spectrum for small α, gives rise to *metastability* [46,53–55]. The evolution $\rho(t) = e^{t\mathcal{L}}\rho_0$ of any initial state ρ_0 can be written in terms of the eigenvalues λ_m and right eigenmatrices R_m of the Liouvillian,

$$\rho(t) = R_0 + \sum_{m=1}^{M} e^{\lambda_m t} c_m R_m + \sum_{m=M+1}^{4^\ell} e^{\lambda_m t} c_m R_m, \qquad (5)$$

where we have split the contribution of the M eigenvalues with largest real parts from the rest of the spectrum, and were the coefficients c_m are given by $c_m = \mathrm{Tr}(L_m\rho_0)$, L_m being the left eigenmatrices. For a large spectral separation, there is a wide range of times for which the modes $m > M$ have already decayed and can be neglected above, giving

$$\rho(t) \approx R_0 + \sum_{m=1}^{M} e^{\lambda_m t} c_m R_m. \qquad (6)$$

This is the metastable regime where dynamics is approximately restricted to the lower-dimensional MM. The valid combinations of c_i classify a MM as either classical or quantum [46,55]. A MM is called *classical* if there exists a basis of density matrices $\tilde{\rho}_i$ so that any state in the MM is a positive linear combination $\rho(t) \approx \sum_{i=1}^{m} p_i\tilde{\rho}_i$ with $0 \leqslant p_i \leqslant 1$. In this case the MM is a simplex, analogous to the manifold of probability distributions, with p_i the probabilities of being in each metastable phase $\tilde{\rho}_i$, and the long-time dynamics can be cast as a classical Markov jump process between these phases. When such basis does not exist the MM is said to be *quantum*.

At the level of the perturbative calculation above, we can read off the eigenmatrices R_m and L_m ($m \leqslant M$) forming the MM. For one good qubit ($\ell_w = 1$), we have three eigenvalues with $n_w = 1, n_s = 0$, and the matrices are the three Pauli strings with a nonidentity on the good qubit and the identity. For two good qubits, we obtain two eigenvalue clusters in the MM, which remain well separated even for large ℓ (cf. discussion in [44] and [52]): one is formed by the six one-qubit Pauli strings with one identity on one of the good qubits ($n_w = 1$), and the other by the nine two-qubit Pauli strings with nonidentities on both good qubits ($n_w = 2$). Perturbation theory thus suggests that the MM is quantum, since it is invariant under the action of SU(2) operators on the slow sites. However, this assumption might fail when we take into account the full random K matrix, the additional corrections allowing for a classical manifold to form. We now test this numerically.

To test for classicality of the MM we apply the algorithmic approach of Refs. [54,55] which tries to systematically find the best possible simplex from spectral data of the Liouvillian. Accuracy is measured by a bound on the average distance of metastable states outside this optimal simplex. This bound follows by noting that given some basis $\tilde{\rho}_m$ ($m = 0, \ldots, M$) of the MM [56], there exists a unique dual basis $\tilde{P}_m$ with normalization chosen as $\mathrm{Tr}(\tilde{P}_m\tilde{\rho}_{m'}) = \delta_{mm'}$. Therefore, the coefficients for a state ρ projected to the MM are given by $p_m = \mathrm{Tr}(\tilde{P}_m\rho)$, bounded by the maximum and minimum eigenvalues of $\tilde{P}_m$. These eigenvalues reside between 0 and 1 if the MM is exactly a simplex, and thus classical. How far any eigenvalues $\lambda_j^{(P_m)}$ of the $\tilde{P}_m$ are outside this range defines a classicality measure [55]

$$\mathcal{C} = \frac{1}{2^N}\sum_{m=0}^{M}\sum_{j=1}^{2^N} \max\left[-\lambda_j^{(P_m)}, 0\right]. \qquad (7)$$

Since an exactly classical MM has vanishing $\mathcal{C}$, the more $\mathcal{C}$ departs from zero the farther away from classical the MM is.

With this procedure we construct the simplex approximation to the MM for a set of 1000 realizations of the disorder matrix K at a dissipation rate $\alpha = 10^{-5}$, showing a histogram of $\mathcal{C}$ in Fig. 2(a) (green). We see that the manifold is never classical, $\mathcal{C} \gtrsim 1$, in the disorder realizations we consider. To illustrate this visually, for one sample realization we plot the projections of random pure states onto the metastable manifold against the expectation values of Pauli operators on the slow site in Fig. 2(c): we see that many of these projections fall outside the optimal simplex, and indication that the MM is not classical. In Fig. 2(e), we evolve a few metastable states as they converge toward the stationary state, seeing that some spend time outside the simplex (but still within the quantum MM).

The quantum nature is apparently robust in this random matrix model as suggested by perturbation theory. It is natural to expect that the noncommuting dissipation channels are responsible for the robustness of the quantum MM, e.g., the

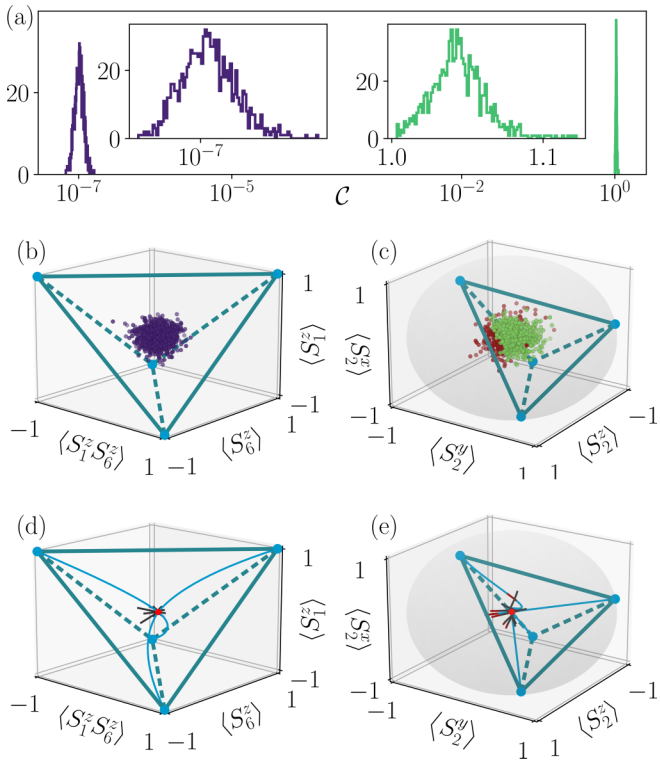

FIG. 2. (a) Histograms of the classicality $\mathcal{C}$ for an ensemble of 1000 disorder realizations of K, for the quantum MM case (green, right) and the classical MM case (purple, left), for $l = 6$ and at a dissipation rate $\alpha = 10^{-5}$. (b) Simplex that best approximates the MM in the classical MM case for one disorder realization (blue dots indicate the extreme metastable phases [56], lines the edges of the simplex, dashed lines are behind the volume of the simplex) in which approximately all metastable states are contained if the MM is classical, in the basis of Pauli strings with Z Pauli matrices on the slow sites 1 and 6 [$S_1^z = S_{z00000}$, $S_6^z = S_{0000z}$, $S_1^z S_6^z = S_{z0000z}$ in the notation of Eq. (1)]. Dots (purple) are projections of a set of random initial states onto the MM, plotted according to the expectation value of the three observables. All states sampled fall within the simplex, as expected for a classical MM. (c) Same for the quantum MM case, now in terms of Pauli strings with a nontrivial Pauli matrix on the slow site [$S_2^x = S_{0x0000}$, $S_2^y = S_{0y0000}$, $S_2^z = S_{0z0000}$]. Projections of random initial states escape the simplex, as the MM is quantum (the shaded Bloch sphere), with those inside colored green and those outside colored red. (d), (e) Projections of the time evolution for long times of the metastable phases (blue curves) and of a set of random initial states (black curves) within the MM toward stationarity (red dot), for the classical MM case (left panel) and quantum MM case (right panel). Curve segments colored red in (e) are outside the simplex approximation.

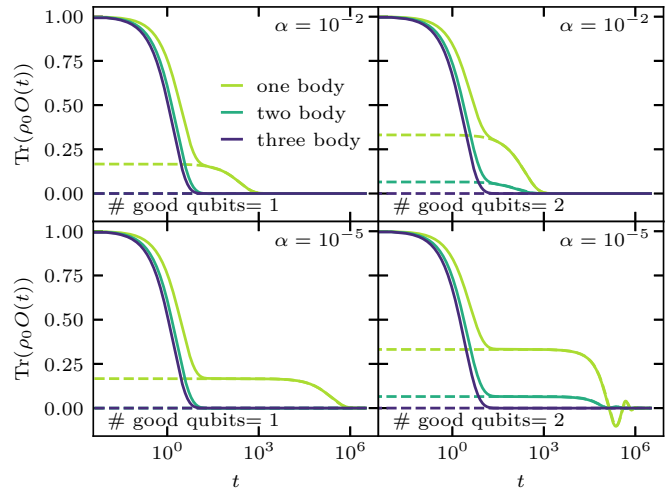

FIG. 3. Comparison of the exact dynamics (solid lines) with the dynamics projected onto the MM (dashed lines) for $\ell = 7$, for qubits with one (left column) and two good (right column) qubits at two different dissipation rates $\alpha = 10^{-2}, 10^{-5}$. We show expectation values of three observables with different localities, each prepared by a random linear superposition of all the Pauli matrices of the corresponding locality. Observables supported by the bad qubits vanish rapidly, and the long-time dynamics on the good qubits coincide with the effective dynamics. Note that for a MM to display, the locality of the observable has to be smaller or equal to the number of the good qubits.

long-time dynamics for $\ell_w = 1$ lives on a Bloch sphere, which a classical master equation cannot approximate. To construct a classical MM, we manually remove this feature by making only the z direction of the good qubits strongly dissipative, i.e., the dissipation rate $\sqrt{\alpha} = 1$ for the Z Pauli matrices on good qubits. For example, we consider this modified model for $\ell_w = 2$, and $\{L_\mu^w\}$ are those jump operators that have X or Y Pauli matrices on the good qubits, but not those with Z. Counterintuitively, the MM is spanned by the strongly dissipative Z Pauli strings on the good qubits because such strings commute with all rapidly relaxing operators in Eq. (3). In this case, the MM is thus made up of 4 operators: the identity, the Z operator on each good qubit, and the product of Z operators on both good qubits. The algorithms of [54,55] yield an extremely accurate simplex approximation to the MM, confirming that it is effectively classical as shown in Fig. 2(a). This is visualized by projecting a set of random states onto the slow-mode eigenspace in Fig. 2(b), locating them well within the simplex. Further, as shown in Fig. 2(d), the long-time evolution of a set of these metastable states (black), or the metastable phases (blue), remains within the simplex at all times.

Metastable dynamics. Using Eq. (5), we can calculate the evolution of observables at any time. To consider generic initial states we choose ρ_0 as a random linear superposition of the full Hilbert space. Figure 3 (full lines) shows the time evolution of observables with different locality properties (nontrivial Pauli strings of different lengths k). Note the appearance of plateaus in the relaxation curves, specifically for the shorter Pauli strings which have a larger overlap with the matrices R_m that define the MM.

After a fast transient, dynamics is confined to the MM. The approximate dynamics is then obtained by projecting both the initial state and the observables onto it, and solving Eq. (6). The dashed curves in Fig. 3 show the corresponding results: the effective dynamics captures the long-time behavior accurately, showing that metastability implies dimensional reduction from the whole Hilbert space to the MM.

Conclusion. Starting from a random local and purely dissipative Liouvillian, we have defined a random matrix model for generic metastability in open quantum systems relevant for strongly varying dissipation timescales in quantum computers if dissipation is strongly dominant. We find that a separation of dissipation timescales induces the presence of a metastable manifold to which initial states relax, before the evolution to the steady state occurs at much longer times. If the dissipation on good qubits does not further single out certain Pauli operators, we show that the metastable manifold is generically quantum, while further structure can lead to classical manifolds instead.

Acknowledgments. This work was supported in part by the Deutsche Forschungsgemeinschaft through SFB 1143 (Project ID 247310070) and the cluster of excellence ML4Q (EXC 2004). J.P.G. and D.C.R. acknowledge financial support from EPSRC Grant No. EP/R04421X/1 and Leverhulme Trust Grant No. RPG-2018-181.

[1] E. P. Wigner, Characteristic vectors of bordered matrices with infinite dimensions, Ann. Math. **62**, 548 (1955).
[2] E. P. Wigner, Random matrices in physics, SIAM Rev. **9**, 1 (1967).
[3] F. J. Dyson, Statistical theory of the energy levels of complex systems. I, J. Math. Phys. **3**, 140 (1962).
[4] F. J. Dyson, Statistical theory of the energy levels of complex systems. II, J. Math. Phys. **3**, 157 (1962).
[5] F. J. Dyson, Statistical theory of the energy levels of complex systems. III, J. Math. Phys. **3**, 166 (1962).
[6] M. L. Mehta, *Random Matrices* (Elsevier, 2004).
[7] M. Feingold, N. Moiseyev, and A. Peres, Ergodicity and mixing in quantum theory. II, Phys. Rev. A **30**, 509 (1984).
[8] J. M. Deutsch, Quantum statistical mechanics in a closed system, Phys. Rev. A **43**, 2046 (1991).
[9] J. M. Deutsch, Eigenstate thermalization hypothesis, Rep. Prog. Phys. **81**, 082001 (2018).
[10] M. Srednicki, Chaos and quantum thermalization, Phys. Rev. E **50**, 888 (1994).
[11] M. Srednicki, Thermal fluctuations in quantized chaotic systems, J. Phys. A: Math. Gen. **29**, L75 (1996).
[12] M. Rigol, V. Dunjko, and M. Olshanii, Thermalization and its mechanism for generic isolated quantum systems, Nature (London) **452**, 854 (2008).
[13] L. D'Alessio, Y. Kafri, A. Polkovnikov, and M. Rigol, From quantum chaos and eigenstate thermalization to statistical mechanics and thermodynamics, Adv. Phys. **65**, 239 (2016).
[14] F. Borgonovi, F. M. Izrailev, L. F. Santos, and V. G. Zelevinsky, Quantum chaos and thermalization in isolated systems of interacting particles, Phys. Rep. **626**, 1 (2016).
[15] M. V. Berry, M. Tabor, and J. M. Ziman, Level clustering in the regular spectrum, Proc. R. Soc. A **356**, 375 (1977).
[16] T. Kinoshita, T. Wenger, and D. S. Weiss, A quantum Newton's cradle, Nature (London) **440**, 900 (2006).
[17] M. Rigol, V. Dunjko, V. Yurovsky, and M. Olshanii, Relaxation in a Completely Integrable Many-Body Quantum System: An *Ab Initio* Study of the Dynamics of the Highly Excited States of 1D Lattice Hard-Core Bosons, Phys. Rev. Lett. **98**, 050405 (2007).
[18] T. Langen, S. Erne, R. Geiger, B. Rauer, T. Schweigler, M. Kuhnert, W. Rohringer, I. E. Mazets, T. Gasenzer, and J. Schmiedmayer, Experimental observation of a generalized Gibbs ensemble, Science **348**, 207 (2015).
[19] P. W. Anderson, Absence of diffusion in certain random lattices, Phys. Rev. **109**, 1492 (1958).
[20] D. M. Basko, I. L. Aleiner, and B. L. Altshuler, Metal-insulator transition in a weakly interacting many-electron system with localized single-particle states, Ann. Phys. **321**, 1126 (2006).
[21] V. Oganesyan and D. A. Huse, Localization of interacting fermions at high temperature, Phys. Rev. B **75**, 155111 (2007).
[22] M. Žnidarič, T. Prosen, and P. Prelovšek, Many-body localization in the Heisenberg *XXZ* magnet in a random field, Phys. Rev. B **77**, 064426 (2008).
[23] A. Pal and D. A. Huse, Many-body localization phase transition, Phys. Rev. B **82**, 174411 (2010).
[24] D. J. Luitz, N. Laflorencie, and F. Alet, Many-body localization edge in the random-field Heisenberg chain, Phys. Rev. B **91**, 081103(R) (2015).
[25] R. Nandkishore and D. A. Huse, Many-body localization and thermalization in quantum statistical mechanics, Annu. Rev. Condens. Matter Phys. **6**, 15 (2015).
[26] D. A. Abanin, E. Altman, I. Bloch, and M. Serbyn, Colloquium: Many-body localization, thermalization, and entanglement, Rev. Mod. Phys. **91**, 021001 (2019).
[27] D. J. Luitz and Y. Bar Lev, Anomalous Thermalization in Ergodic Systems, Phys. Rev. Lett. **117**, 170404 (2016).
[28] D. J. Luitz and Y. Bar Lev, The ergodic side of the many-body localization transition, Ann. Phys. **529**, 1600350 (2017).
[29] D. A. Abanin and Z. Papić, Recent progress in many-body localization, Ann. Phys. **529**, 1700169 (2017).
[30] V. Khemani, A. Lazarides, R. Moessner, and S. L. Sondhi, Phase Structure of Driven Quantum Systems, Phys. Rev. Lett. **116**, 250401 (2016).
[31] D. V. Else, B. Bauer, and C. Nayak, Floquet Time Crystals, Phys. Rev. Lett. **117**, 090402 (2016).
[32] V. Khemani, R. Moessner, and S. L. Sondhi, A brief history of time crystals, arXiv:1910.10745.
[33] H. Bernien, S. Schwartz, A. Keesling, H. Levine, A. Omran, H. Pichler, S. Choi, A. S. Zibrov, M. Endres, M. Greiner, V. Vuletić, and M. D. Lukin, Probing many-body dynamics on a 51-atom quantum simulator, Nature (London) **551**, 579 (2017).
[34] C. J. Turner, A. A. Michailidis, D. A. Abanin, M. Serbyn, and Z. Papić, Weak ergodicity breaking from quantum many-body scars, Nat. Phys. **14**, 745 (2018).
[35] N. Pancotti, G. Giudice, J. I. Cirac, J. P. Garrahan, and M. C. Bañuls, Quantum East Model: Localization, Nonthermal Eigenstates, and Slow Dynamics, Phys. Rev. X **10**, 021051 (2020).

[36] S. Denisov, T. Laptyeva, W. Tarnowski, D. Chruściński, and K. Życzkowski, Universal Spectra of Random Lindblad Operators, Phys. Rev. Lett. **123**, 140403 (2019).
[37] L. Sá, P. Ribeiro, and T. Prosen, Spectral and steady-state properties of random Liouvillians, J. Phys. A: Math. Theor. **53**, 305303 (2020).
[38] T. Can, Random Lindblad dynamics, J. Phys. A: Math. Theor. **52**, 485302 (2019).
[39] T. Can, V. Oganesyan, D. Orgad, and S. Gopalakrishnan, Spectral Gaps and Midgap States in Random Quantum Master Equations, Phys. Rev. Lett. **123**, 234103 (2019).
[40] S. Lange and C. Timm, Random-matrix theory for the Lindblad master equation, Chaos **31**, 023101 (2021).
[41] J. Ginibre, Statistical ensembles of complex, quaternion, and real matrices, J. Math. Phys. **6**, 440 (1965).
[42] C. Timm, Random transition-rate matrices for the master equation, Phys. Rev. E **80**, 021140 (2009).
[43] W. Tarnowski, I. Yusipov, T. Laptyeva, S. Denisov, D. Chruściński, and K. Życzkowski, Random generators of Markovian evolution: A quantum-classical transition by superdecoherence, Phys. Rev. E **104**, 034118 (2021).
[44] K. Wang, F. Piazza, and D. J. Luitz, Hierarchy of Relaxation Timescales in Local Random Liouvillians, Phys. Rev. Lett. **124**, 100604 (2020).
[45] O. E. Sommer, F. Piazza, and D. J. Luitz, Many-body hierarchy of dissipative timescales in a quantum computer, Phys. Rev. Research **3**, 023190 (2021).
[46] K. Macieszczak, M. Guţă, I. Lesanovsky, and J. P. Garrahan, Towards a Theory of Metastability in Open Quantum Dynamics, Phys. Rev. Lett. **116**, 240404 (2016).
[47] H. Fröml, A. Chiocchetta, C. Kollath, and S. Diehl, Fluctuation-Induced Quantum Zeno Effect, Phys. Rev. Lett. **122**, 040402 (2019).
[48] S. Wolff, A. Sheikhan, S. Diehl, and C. Kollath, Nonequilibrium metastable state in a chain of interacting spinless fermions with localized loss, Phys. Rev. B **101**, 075139 (2020).
[49] C. Gardiner and P. Zoller, *Quantum Noise* (Springer, 2004).
[50] Note that we do not impose a notion of geometry, essentially dealing with a zero-dimensional system. A geometry can be added on top as discussed in the Supplemental Material of Ref. [44], and adds further complexity, which we do not discuss here to focus on the essential physics of metastability.
[51] Note that the normalization is automatic since we defined Pauli strings such that $\mathrm{Tr}S_\mu^2 = 1$.
[52] See Supplemental Material at http://link.aps.org/supplemental/10.1103/PhysRevB.105.L180201 for an analysis of the system size dependence of the eigenvalue cluster locations and widths, using numerical results from degenerate perturbation theory, and a demonstration of the survival of the metastable manifold in the thermodynamic limit for a fixed number of good qubits. It also provides a figure demonstrating the spectrum of the Liouvillian in the classical metastable manifold case.
[53] D. C. Rose, K. Macieszczak, I. Lesanovsky, and J. P. Garrahan, Metastability in an open quantum Ising model, Phys. Rev. E **94**, 052132 (2016).
[54] D. C. Rose, K. Macieszczak, I. Lesanovsky, and J. P. Garrahan, Phys. Rev. E **105**, 044121 (2022).
[55] K. Macieszczak, D. C. Rose, I. Lesanovsky, and J. P. Garrahan, Theory of classical metastability in open quantum systems, Phys. Rev. Research **3**, 033047 (2021).
[56] The states $\tilde{\rho}_m$ are called "extreme metastable states" [55]. They define the vertices of the simplex that best approximates a classical MM, and all metastable states are probabilistic mixtures of them. They correspond to the "metastable phases" that coexist during the long transient regime of metastability.